AD-A159 196 EXPERIMENTAL INVESTIGATION OF ALUMINUM COMBUSTION IN SULFUR HEXAFLUORIDE ATMOSPHERE(U) NAVAL POSTGRADUATE SCHOOL MONTEREY CA J KOL ET AL. JUL 85 NPS67-85-001CR 1/1

UNCLASSIFIED N62271-84-M-3357 F/G 21/2 NL

END

FILMED

DTIC

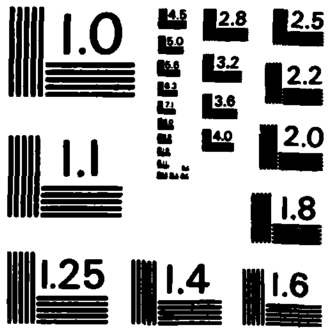

MICROCOPY RESOLUTION TEST CHART
NATIONAL BUREAU OF STANDARDS-1963-A

(2)

NPS67-85-001CR

NAVAL POSTGRADUATE SCHOOL
Monterey, California

CONTRACTOR REPORT

EXPERIMENTAL INVESTIGATION OF ALUMINUM COMBUSTION IN SULFUR HEXAFLUORIDE ATMOSPHERE

Jacob Kol and Yair Chozev

July 1985

Approved for public release; distribution unlimited.

Prepared for: Naval Surface Weapons Center
White Oak Labotatories
Silver Springs, MD 20910

NAVAL POSTGRADUATE SCHOOL
Monterey, California

RADM R. H. Shumaker
Superintendent

D. A. Schrady
Provost

The work reported herein was carried out for the Naval Postgraduate School by Mr. Jacob Kol under Contract N62271-84-M-3357 and Mr. Yair Chozev under Contract N62271-84-M-3055. The work presented in this report is in support of "Underwater Shaped Charges" sponsored by the Naval Surface Weapons Center. The work provides experimental data about the combustion of aluminum in sulfur hexafluoride atmosphere. The data includes burning time, velocity and track width of ejected particles from exploding wire and it is compared to combustion of aluminum in air and steam atmospheres. The project at the Naval Postgraduate School is under the cognizance of Distinguished Professor A. E. Fuhs who is principal investigator.

Prepared by:

MR. YAIR CHOZEV
Research Contractor

MR. JACOB KOL
Research Contractor

Reviewed by:

Allen E Fuhs

ALLEN E. FUHS
Distinguished Professor

M. F. Platzer

M. F. PLATZER
Chairman, Department of Aeronautics

Released by:

J N Dyer

J. N. DYER
Dean of Science and Engineering

UNCLASSIFIED

SECURITY CLASSIFICATION OF THIS PAGE (When Data Entered)

REPORT DOCUMENTATION PAGE

READ INSTRUCTIONS BEFORE COMPLETING FORM

1. REPORT NUMBER: NPS67-85-001CR	2. GOVT ACCESSION NO.: AD-A159196
3. RECIPIENT'S CATALOG NUMBER	
4. TITLE (and Subtitle): Experimental Investigation of Aluminum Combustion in Sulfure Hexafluoride Atmosphere	5. TYPE OF REPORT & PERIOD COVERED: Contractor's Report, April 1985 - July 1985
	6. PERFORMING ORG. REPORT NUMBER
7. AUTHOR(s): Jacob Kol and Yair Chozev	8. CONTRACT OR GRANT NUMBER(s): N62271-84-M-3357, N62271-84-M-3055
9. PERFORMING ORGANIZATION NAME AND ADDRESS: Naval Postgraduate School, Monterey, CA 93943-5100	10. PROGRAM ELEMENT, PROJECT, TASK AREA & WORK UNIT NUMBERS
11. CONTROLLING OFFICE NAME AND ADDRESS	12. REPORT DATE: July 1985
	13. NUMBER OF PAGES: 37
14. MONITORING AGENCY NAME & ADDRESS (if different from Controlling Office): Naval Postgraduate School, Monterey, CA 93943-5100	15. SECURITY CLASS. (of this report): UNCLASSIFIED
	15a. DECLASSIFICATION/DOWNGRADING SCHEDULE

16. DISTRIBUTION STATEMENT (of this Report)

Approved for public release; distribution unlimited.

Accession For	
NTIS GRA&I	☒
DTIC TAB	☐
Unannounced	☐
Justification	
By	
Distribution/	
Availability Codes	
Dist	Avail and/or Special
A-1	

17. DISTRIBUTION STATEMENT (of the abstract entered in Block 20, if different from Report)

18. SUPPLEMENTARY NOTES

DTIC COPY INSPECTED 3

19. KEY WORDS (Continue on reverse side if necessary and identify by block number)

Combustion, Burning, Burning Time, Combustion of Metal, Burning of Metal, Combustion in Steam, Burning in Steam, Aluminum Sulfur Hexafluoride

20. ABSTRACT (Continue on reverse side if necessary and identify by block number)

The goal of this report is to summarize the experimental results and studies of aluminum combustion in sulfur hexafluoride atmosphere. The particles has been ejected from exploding wire. Using photography, burning time, particle size, velocity, deceleration, and temperature were measured. Typical results are as follows: 380 ± 25 micron diameter; particles burn in 10 ± .75 ms; the average initial velocities were from 10 m/s to 15 m/s; the average decelerations were from 4000 m/s^2 to 8000 m/s^2. The average

DD FORM 1 JAN 73 1473 EDITION OF 1 NOV 65 IS OBSOLETE

S N 0102-LF-014-6601

UNCLASSIFIED

SECURITY CLASSIFICATION OF THIS PAGE (When Data Entered)

temperature of the burning particle was 2750 ± 150 K. According to the burning studies of the particles and the measured temperature results the mechanism of burning can be surface burning or vapor phase burning that occurs close to the surface of the hot particle.

TABLE OF CONTENTS

LIST OF FIGURES

LIST OF TABLES

ABSTRACT

The goal of this report is to summarize the experimental results and studies of aluminum combustion in sulfur hexafluoride atmosphere. The particles has been ejected from exploding wire. Using photography, burning time, particle size, velocity, deceleration, and temperature were measured. Typical results are as follows: 380 ± 25 micron diameter; particles burn in 10 ± .75 ms; the average initial velocities were from 10 m/s to 15 m/s; the average decelerations were from 4000 m/s^2 to 8000 m/s^2. The average temperature of the burning particle was 2750 ± 150 K. According to the burning studies of the particles and the measured temperature results the mechanism of burning can be surface burning or vapor phase burning that occurs close to the surface of the hot particle.

ACKNOWLEDGEMENT

The authors acknowledge the valuable help, cooperation and guidance of Professor Allen E. Fuhs during this work.

I. INTRODUCTION

The number of research efforts involving sulphur hexafluoride reaction with electrically exploded aluminum wires is very small. Consequently, one rarely finds published literature on the topic. The SF_6 gas has high thermal stability and its stability in presence of exploding high temperature metal particles was unknown. To investigate stability of SF_6, Cook et. al. [1], performed the studies of electrically exploded Al, Zr, Ag and Pt wires in SF_6 atmosphere by using discharge capacitors as the source of electrical energy. They found that the reaction is highly exothermic creating SF_4 products in the reaction. Grigor'eva et. al. [2], summarized their studies by stating that the exposure of the liquid aluminum to SF_6 passivates the oxide film of the metal surface. Their results indicate that the oxide film will not grow in the presence of SF_6. Measured values of the burning time, velocity variations, wire rupture energy, temperature, aerodynamic drag and the reaction behavior of aluminum particles in different atmospheres are summarized in this report.

II. DESCRIPTION OF THE EXPERIMENTS

A. Experimental Procedure

The experiments were conducted in pressure vessel which consisted of a twelve-inch high stainless steel cylinder, 10.75 inches diameter with four evenely spaced, five-inch diameter observation ports welded into its circumference. One-inch thick, Schlieren quality, borosicalate crown glass (BK-7) was installed in each port. Two Watlow Band Heaters were used to heat the apparatus to operating temperature and four additional Watlow Heaters were mounted on observation ports in order to prevent steam condensation during experiments. An Omega model 157 Digital Controller was used for temperature stabilization. The experiments were conducted in pressure range of 20 to 21 psi and temperature of 85°C. Thermocouples were mounted in different locations inside the chamber to measure the internal temperature.

B. Electrical Energy Measurements for Wire Rupture

The aluminum particles were generated by the exploding wire technique. The 5 cm length wire was mounted between two holders, and the energy transferred to the wire to cause rupture was about 58 Joule. The direct energy measurements included the calibrated shunt current measurement and direct voltage measurements across the wire as shown in Fig. 1.

C. Particle Temperature Measurements

Particle temperature was measured by two-color photo-pyrometry method (see Berger, et. al., [3]). An Optronics Microdensitometer Photoscan system P-1000 was used for optical density measurements. Two still Pentax 35 mm cameras were used for two-color (480 nm, 650 nm) photography of the events. Kodak 2475 recording film was calibrated for a detailed graph of film density versus exposure. One millimeter aluminum wire with purity of 99.998% was used in the experiments.

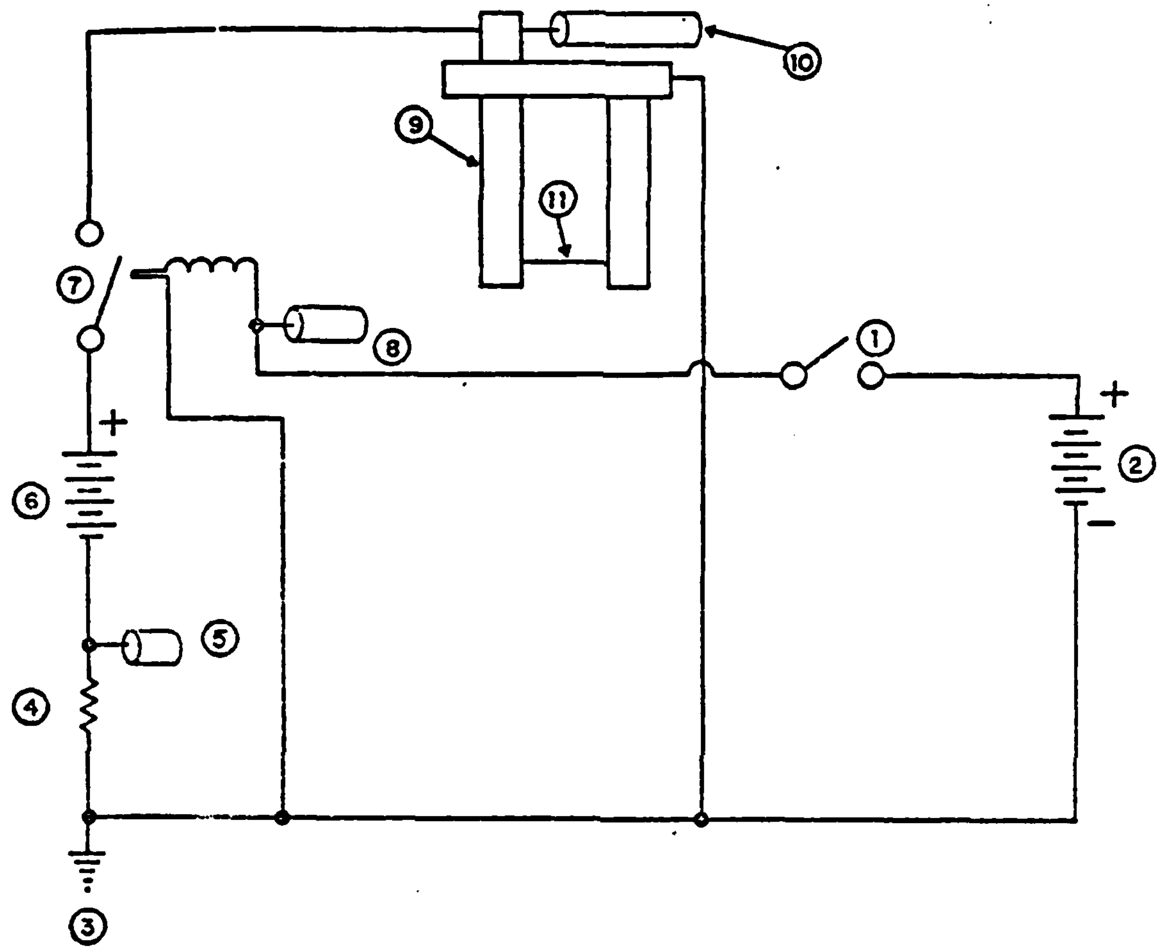

Figure 1. Diagram of Test Wire Circuit

(1) Firing switch, (2) 12 Volt battery; provided e ectrical energy for firing switch, (3) Common ground point for entire circuit, (4) Shunt, (5) Coaxial cable to measure current throught the wire, (6) 12 Volt battery; provided electrical energy for test wire, (7) Solenoid, (8) Coaxial cable to trigger wave-form recorder, (9) Test wire holder assembly, (10) Coaxial cable to measure voltage across wire, (11) Aluminum test wire.

D. Particle Burning Time Measurements

Particle burning time was measured using 35 mm still camera equipped with high speed light chopper; see Chozev et. al. [4]. Kodak Ektachrome 200 ASA film was used for photography of the time events along the particle track. The chopper period was measured to be 0.77 ms while the on to off ratio is 2. Hence, the exposure time is 0.77 x 2/3 = 0.51 ms. Elapsed time or burning time is measured using the number of chopper periods.

E. Measurement of Particle Velocity and Deceleration

The particle velocity variations along the particle track were performed using two 35 mm still cameras as shown in Fig. 2. Using the r, α, β and data from the photographs one can find the velocity equation, $v(t)$, as follows:

$$v(t) = \frac{\Delta r(t)}{\Delta T} \sqrt{1 + \tan\beta \cos\alpha} \tag{1}$$

where $\Delta r(t)$ is the length of chopped segment of the particle track. ΔT is chopper period (0.77 ms). β is the inclination angle as is seen at the camera 2. α is the angle as is seen at camera 1.

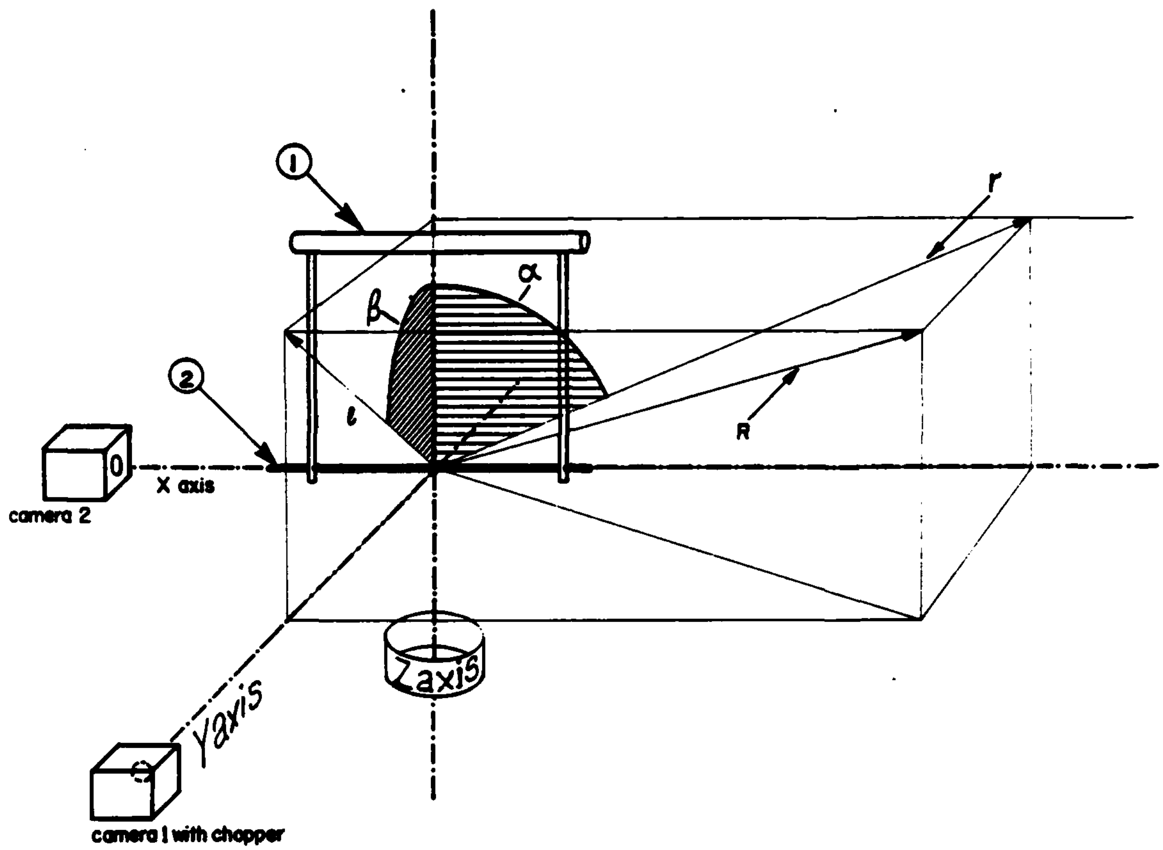

Figure 2. Arrangement for Velocity Measurements

(1) Holder, (2) Wire, r = distance of the track on exposured film of camera 1, α = angle of the track relative to perpendicular axis on the exposure of camera 1, β = angle of the inclination of the particle track on the exposure of camera 2, R = real distance of the particle track.

III. RESULTS

A. Photographs of Aluminum Exploding Wire in SF_6 Atmosphere

The typical behavior of aluminum wire rupture and subsequent combustion in SF_6 atmosphere is photographed using 35 mm Pentax camera and is shown in Fig. 3.

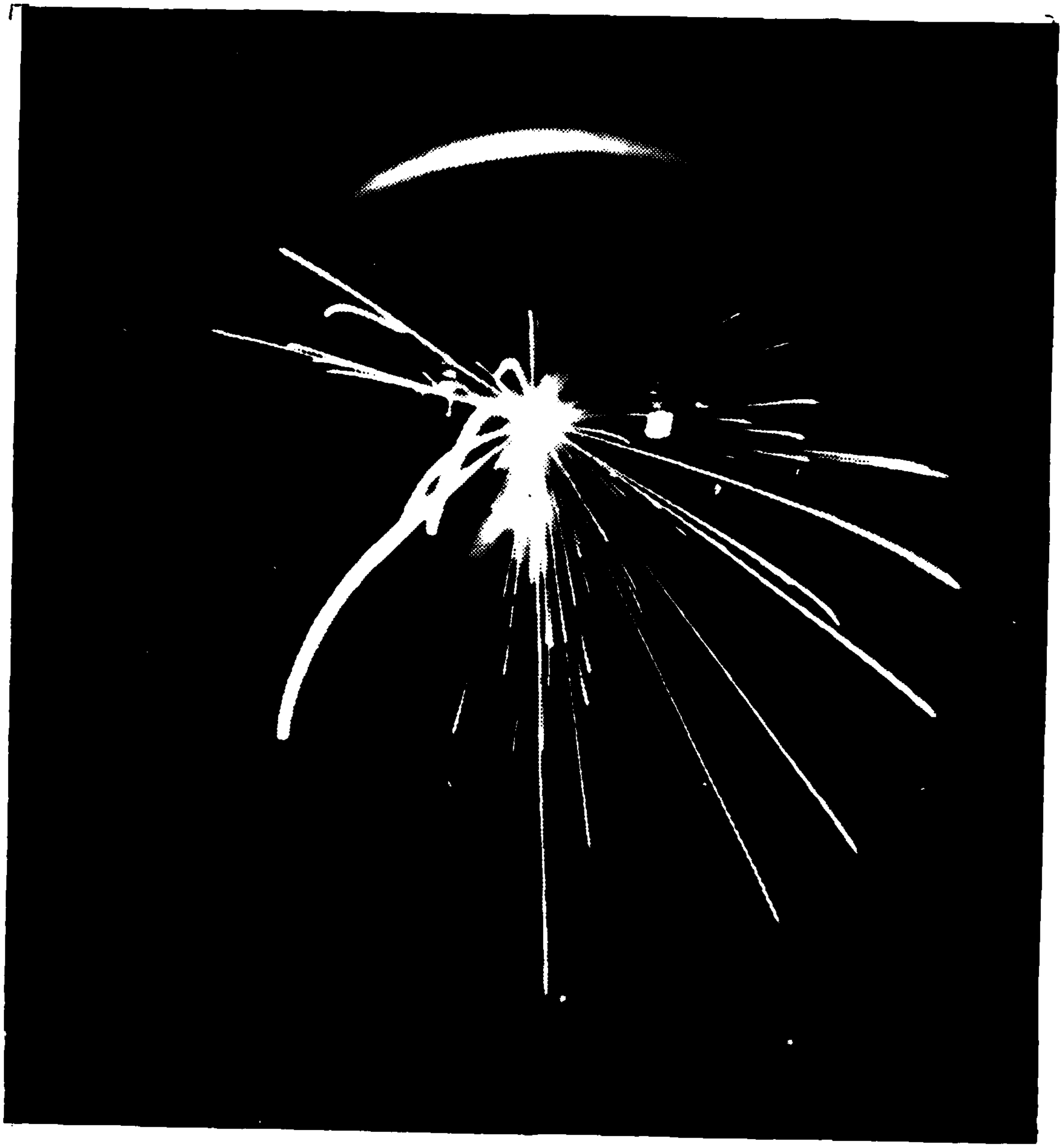

Figure 3. Aluminum Wire Combustion in SF_6 Atmosphere

Fig. 3 shows the following behavior of the plasma and the particles after the explosion:

1. <u>Plasma</u>

   The size of the plasma varies from 0.5 to 0.8 cm in diameter while the color of the glow around the plasma was between blue and violet. A few blue streaks radiate from the plasma.

2. <u>Particles</u>

   A relatively large number of particles were ejected from the plasma (30 to 140). The tracks were characterized by light red illumination while the film exposure is weaker at the ejection region due to higher velocities of the particles.

B. Burning Time Measurements

The burning time measurements were performed by using the photograph from camera 1 described in Fig. 2. The burning times of aluminum particles in SF_6 atmosphere varies from 9 to 77 ms. Table 1 has burning rate data for two particles. Given in Table 1 are two columns for time and for track width. The precise relation between particle radius and track width is unknown. Certainly the particle radius is less than the track width. A burning particle surrounded by a flame may yield a track width equal to diameter for the flame. Table 1 indicates that a particle with a track width of 0.285 mm has a burning time of 9.24 ms; likewise a track width of 0.302 mm results in a burning time of 12.52 ms.

C. Velocity and Deceleration Measurements

The velocity and deceleration measurements were performed by using photography with 35 mm still cameras. One camera was equipped with a light chopper, and an additional camera was positioned perpendicular to the first

camera for measurement of inclination angles as described in Fig. 2. By using equation (1) and distance calibration, the velocity and deceleration of two representative particles are summarized in Table 1. The same particle tracks are shown in Fig. 4a and Fig. 4b as photographed by the two cameras in Fig. 2.

D. Particle Size Measurements

In Table 1, the size of two representative burning particles are summarized. One can conclude that the size is decreasing along the track from the plasma towards the end of the track.

One would like to have burning time as a function of initial particle size but burning time is affected by particle velocity. To measure particle velocity, the procedure discussed in connection with Fig. 2 must be used.

Table 1. Velocity, Deceleration and Size Variation for two Typical Particles

Track No.	Frame No.	Time (ms)	$\Delta r(t)$ (mm)	Velocity (m/s)	Deceleration ($m/s^2 \times 10^3$)	Track Width (mm)	$-\Delta r_c/\Delta t$ (m/s^2)
1	1	.77	8.49	11.03		.285	
	2	1.54	5.79	7.52	4.56	.285	
	3	2.31	3.67	4.77	3.57	.248	
	4	3.08	2.90	3.77	1.30	.248	8000
	5	3.85	2.12	2.75	1.32	.248	
	6	4.62	1.54	2.00	.97	.242	
	7	5.49	1.35	1.75	.32	N/A	
	8	6.16	1.16	1.51	.31	N/A	
	9	6.93	0.97	1.26	.32	N/A	
	10	7.70	0.77	1.00	.34	N/A	
	11	8.47	0.58	0.75	.32	N/A	
	12	9.24	0.48	0.62	.17	N/A	
2	1	.77	8.73	11.34		.302	
	2	1.54	6.51	8.45	3.75	.302	
	3	2.31	5.15	6.69	2.29	.276	
	4	3.08	4.19	5.44	1.62	.276	
	5	3.85	3.29	4.27	1.52	.276	
	6	4.62	2.78	3.61	.86	.276	4000
	7	5.49	2.38	3.09	.68	.276	
	8	6.16	2.08	2.70	.51	.261	
	9	6.93	1.82	2.36	.44	.261	
	10	7.70	1.60	2.08	.36	.261	
	11	8.47	1.39	1.81	.35	.261	
	12	9.24	1.23	1.60	.27	N/A	
	13	10.01	1.05	1.36	.31	N/A	
	14	10.78	0.93	1.21	.19	N/A	
	15	11.55	0.82	1.06	.19	N/A	
	16	12.32	0.73	0.91	.19	N/A	

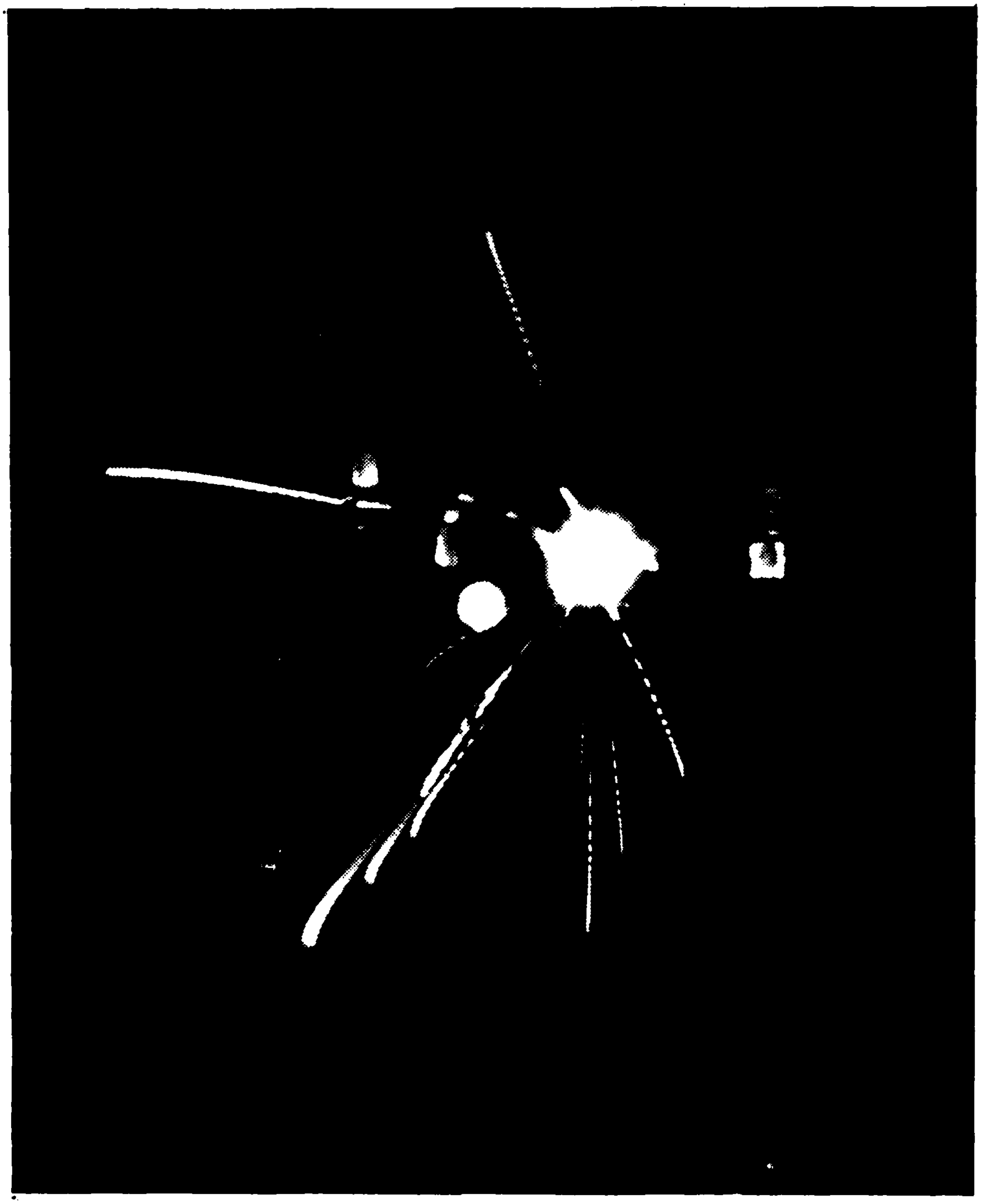

Figure 4a. Event as Photographed by Camera #1 of Figure 2. Note: The broken tracks are due to chopper. Tracks are used to measure angle α .

Figure 4b. Event as Photographed by Camera #2 of Figure 2. Tracks are used to measure angle β .

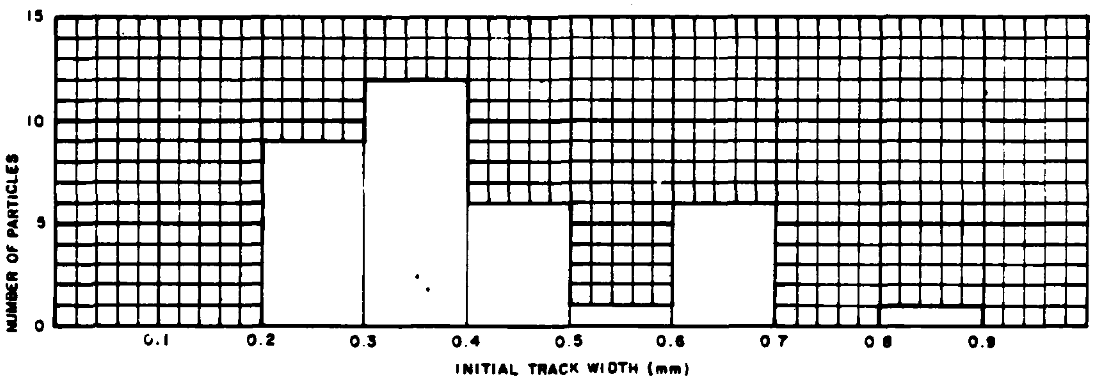

Figure 5a. Histogram of Initital Track Size

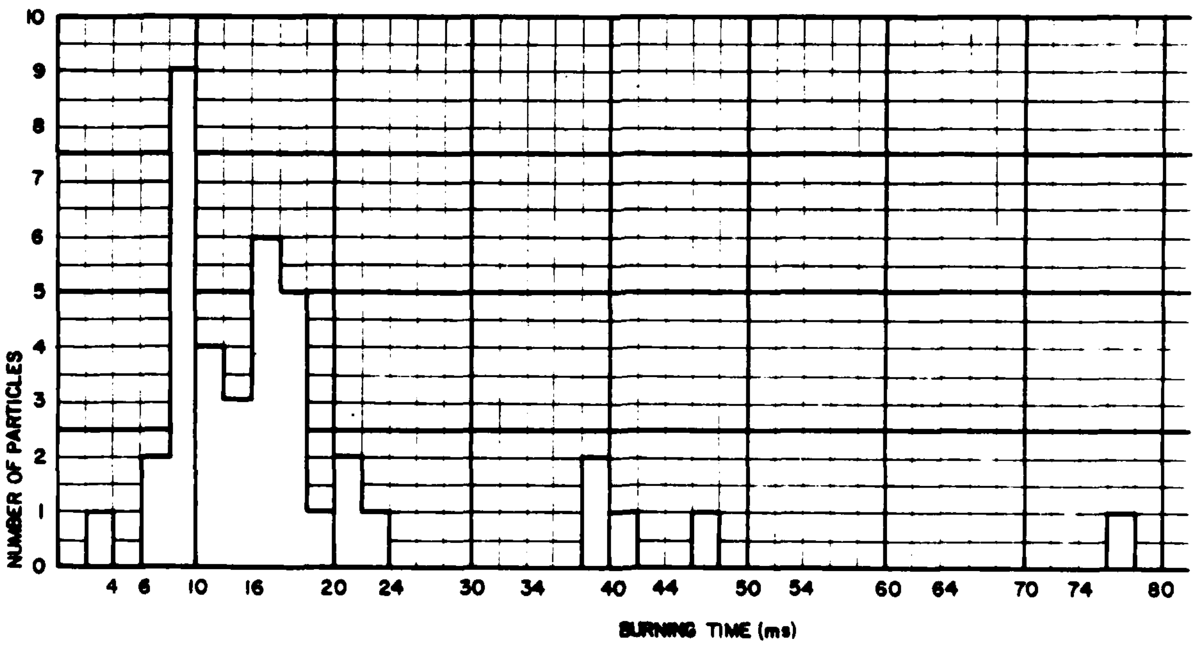

Figure 5b. Histogram of Particle Burning Time

Due to the very large number of particles whose tracks criss-cross, the ability to follow a specific particle is limited.

In lieu of particle burning time as a function of initial particle size, histograms of initial track size and burning time are possible. These histograms are shown in Fig. 5a and Fig. 5b.

E. Measurement of Energy for Wire Rupture

The ignition measurements were performed by using the arrangement as described in Fig. 1. The average rupture energy was 58±3 Joules. The aluminum wire had a diameter of 1.0 mm.

F. Aerodynamic Drag Studies

By using experimental results for the velocity, deceleration, and burning particle size, particle motion can be determined. Application of Newton's second and third laws to the particle yields the following equaiton of motion for particle motion in continuum flow:

$$m \frac{dV}{dt} = -\dot{m}V - F \qquad (2)$$

where

$$F = \frac{1}{2} \rho_g V^2 C_D A$$

Reynolds number, Re , is calculated as follows:

$$Re = \frac{\rho_g Vd}{\mu} = 1000$$

for following values:

μ - viscocity = 23.8×10^{-6} kg/sm [5]
V - initial velocity = 11 m/s
ρ_g - SF_6 density at 366 K = 7.3 kg/m^3
d - particle diameter = 300 μm

Using Hoerner [6] it follows that the particle drag coefficient is about 0.8. By using the assumption that particle mass is $m = \rho_{A\ell} 4\pi r^3/3$ and the aluminum density is constant, equation (2) can be rewritten as follows:

$$\frac{dV}{dt} = -3V\frac{\dot{r}}{r} - 1.5\frac{\rho_g}{\rho_{A\ell}}V^2 C_D \frac{1}{r} \quad (3)$$

The first term (in the right side) in equation (3) represents the mass reduction due to a uniform outward flux of AlF_3 molecules. The net force on the particle due to the flux of AlF_3 is zero. For typical particle of $r = 145\,\mu m$ with initial velocity of $V=11.2$ m/s and average $\dot{r} = -6.10^{-3}$ m/s, the calculated deceleration is 2807 m/s^2 which is comparable with the average measured deceleration 4155 m/s^2. One can conclude therefore that the drag is the cause for the deceleration.

G. Temperature Measurement of Aluminum Particles in SF_6 Atmosphere

The temperature measurements were performed using the two color-photo-pyrometry method (TC-PPM) method as described by Berger et. al., [3]. Typical results for temperature measurements are shown in Fig. 7 and Fig. 9 based on measured film densities that are shown in Fig. 6 and Fig. 8, respectively.

Table 2. Film Density and Calculated Temperature as a Function of Distance Along the Particle Tracks

Distance	D_1	D_2	T_m K
236.0	1.91	1.22	2551 ± 5.7%
222.0	1.92	1.27	2654 ± 5.7%
195.0	1.68	1.04	2513 ± 5.7%
165.0	1.35	.93	2822 ± 5.7%
152.0	.98	.65	2772 ± 5.7%
127.0	1.20	.85	2897 ± 5.7%

Notes:

1. Distance is normalized; actual distance in millimeter is obtained by multiplying by 0.1315.

2. D_1 is the film denstiy using red filter, and D_2 is the film density using the blue filter. These data apply to Fig. 6 and 8.

3. The error of 5.7% was calculated using the procedure of References 3 and 7.

In Fig. 7 and Fig. 9, horizontal lines have been drawn at the vapor temperature for pure aluminum which is 2740 K. The measured particle temperatures are nearly equal to the vapor temperature.

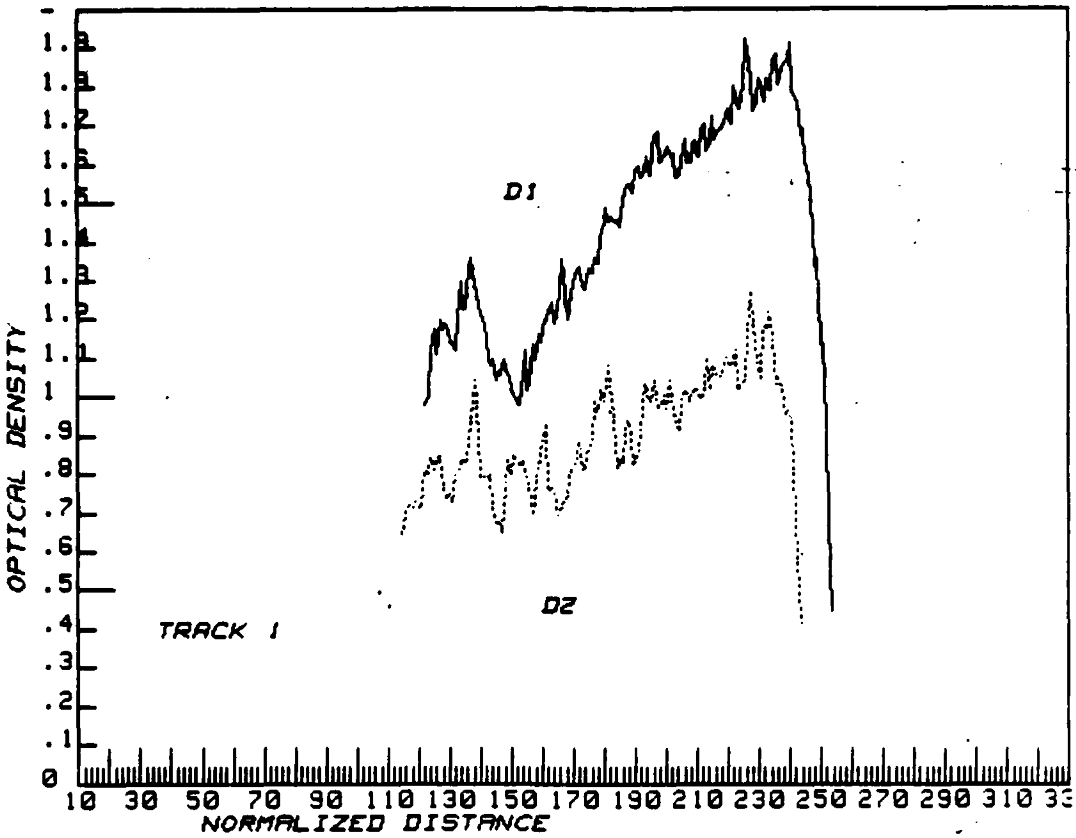

Figure 6. Measured Film Densities Used for Calculating Temperatures Shown in Figure 7.

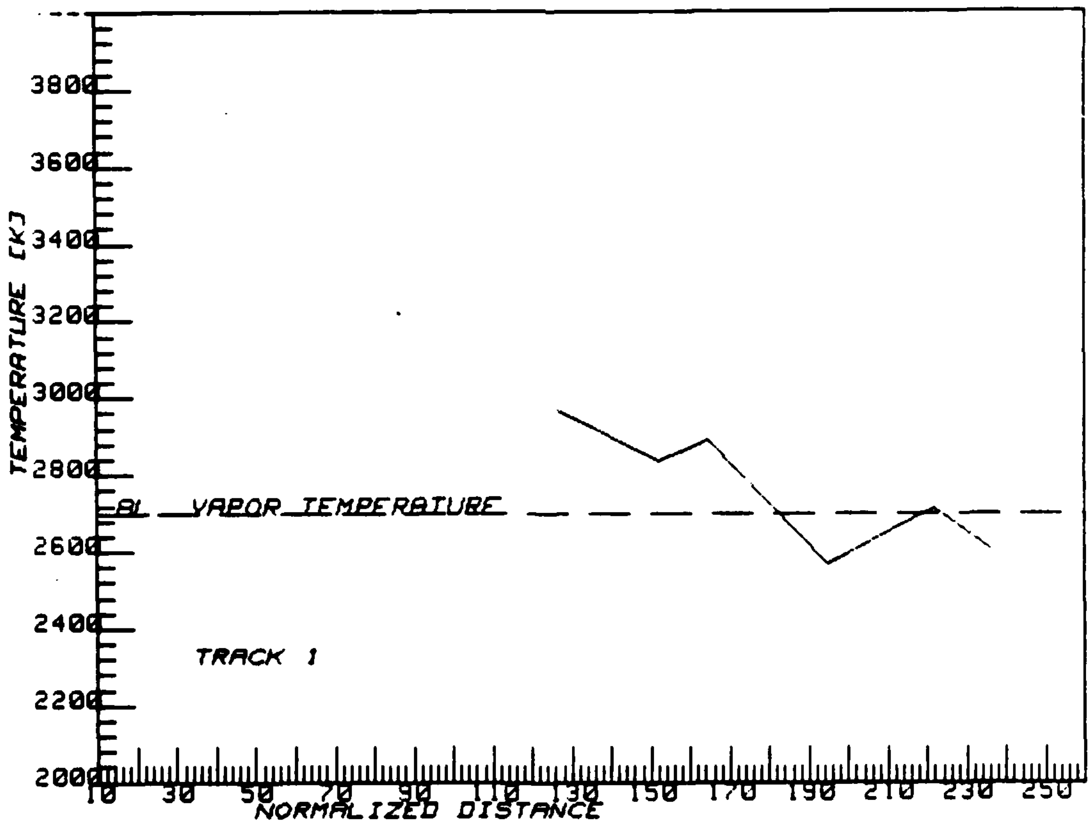

Figure 7. Calculated Temperatures for Typical Track.

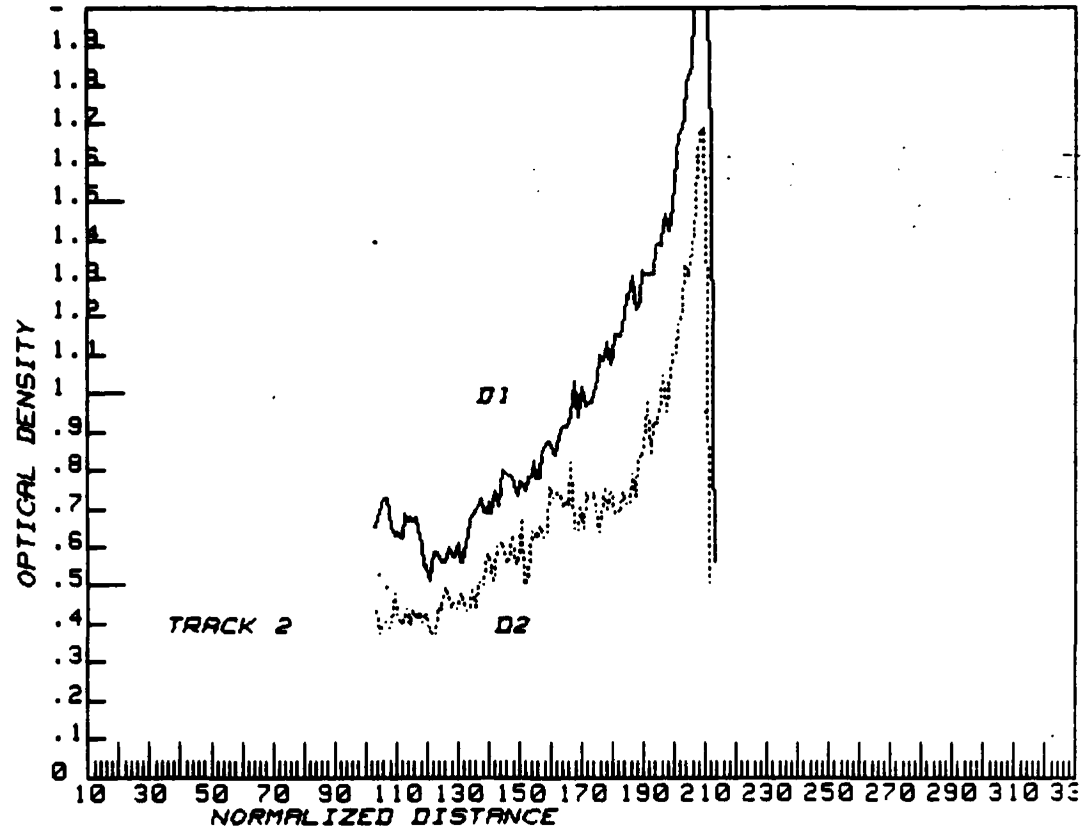

Figure 8. Measured Film Densities Used for Calculating Temperatures Shown in Figure 9.

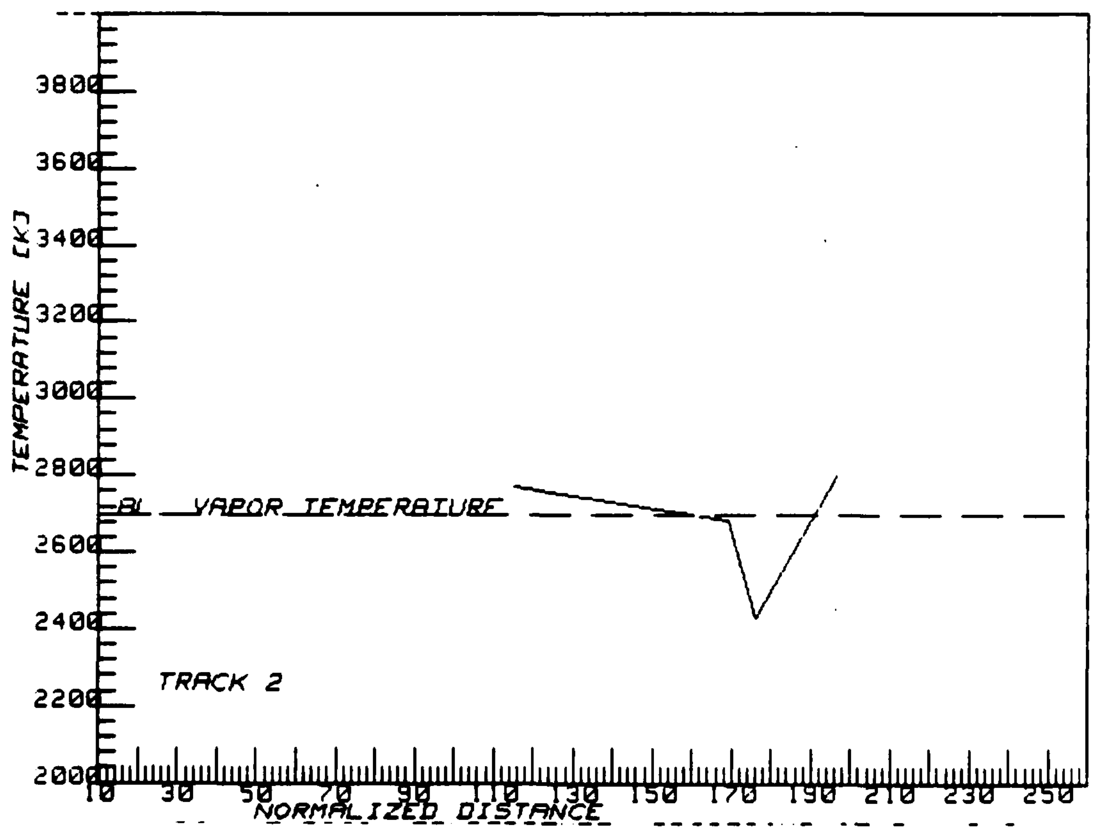

Figure 9. Calculated Temperatures for Typical Track

IV. DISCUSSION

A. A Comparison of Aluminum Combustion in Different Atmospheres

Aluminum vapor reacting in oxygen, steam or SF_6 is exothermic. The heat of reaction for each case is shown in Table 3.

Experimental results are reported in Table 4. Each of the column headings will be discussed. In addition to combustion in air, steam and SF_6 tests were conducted in vacuum.

Motivation for conducting the tests in vacuum included the desire to ascertain the influence of ambient atmosphere on wire rupture. Also the radiation from particle should not be the same in vacuum since combustion does not occur.

Table 3. Heat of Reaction for Aluminum Reacting with Oxygen, Steam and Sulfur Hexafluoride

Ambient Gas	Reaction kcal/mole	ΔH(298 K) kcal/mole
Oxygen	$2Al(g) + 3/2\ O_2\ (g) \rightarrow Al_2O_3$	-408
Steam	$2Al(g) + 3H_2O(g) \rightarrow Al_2O_3 + 3H_2$	-237
SF_6	$2Al(g) + 3SF_6\ (g) \rightarrow 2AlF_3 + 3SF_4$	-264

Notes: The value of ΔH shown is the kcal/mole of product, i.e., Al_2O_3 or AlF_3 as appropriate.

The electrical energy input to the wires was measured. The energy input causes rupture of the wire and establishes the initial conditions for the ejected particles. These initial conditions include number of particles, size distribution of particles, initial temperature, and particle velocity.

In magnitude, the energy to cause rupture is 86 J for air atmosphere decreasing to 58 J for SF_6 atmosphere.

Table 4. Aluminum Wire Combustion in Different Gas Atmospheres

Ambient Gas	Experimental Wire Rupture Energy (Joules)	Number of Particles	Average Time Particle Radiates (ms)	Velocity (m/s)	Plasma Description	Particle Behavior	Average Track Width (mm)
Air	86	28-50	<6>	6-20	1cm in size white plasma with 0.29cm blue glow around plasma.	Big particles recognize with bright path, while small particles light red Most of the particle behaved with erratic trajectories.	N/A
Steam	73	35-40	<4>	20-26	0.4cm in size plasma with white color at the center, 1.4 to 2.2cm purple glow around the plasma.	All particles had bright path from the begining. Most of the particles ended with super-cooling effect, some had spinning.	0.73
Vacuum	N/A	7-32	<21>	3-8	1.8-1.2cm in size white plasma, 0.12cm in width blue glow around the plasma.	The color of the path is light red almost unseen.	N/A
SF_6	58	30-140	<10>	10-15	0.5-0.8cm white in size plasma, 0.9cm in width purple glow around the plasma.	The particles had straight light red tracks. At the begining there is an interupt in exposure.	0.38

To explain the difference the following arguments can be made: the wire initially has a thin coating of aluminum oxide. The aluminum oxide has a higher melting temperature (2300 K) than pure aluminum (932 K). In either air or steam as the wire is heated, the oxide layer grows in thickness. In contrast, as the wire is heated in SF_6 an increase in thickness of oxide layer does not occur. The oxide layer provides mechanical strength as well as absorbs more energy due to higher melting temperature. These observations are consistent with the observations of Brzustowski and Glassman [8] and Grigor'eva [2].

For each of many individual tests of exploding wires, the number of particles created by the wire rupture were counted. The range of particle counts are given in each case. The number of particles formed by wire rupture in vacuum is considerably less than for rupture in air or steam. Further, many more particles may be formed by wire rupture in SF_6. Hence the ambient gas influences wire rupture.

The missing segment of wire, which forms the hot particles, tends to be about one wire diameter. Knowing the wire "gap" and number of particles, an estimate can be made for average particle diameter.

In passing, a comment concerning the radiation from particles formed in vacuum and in an oxidizing atmosphere is appropriate. When the particle is formed in vacuum, the radiant energy which exposes the film is due solely to thermal radiation. For burning particles the radiation includes that due to chemical reaction in the flame. To observe the particles formed in vacuum, the most sensitive film (ASA 3200) was required. For observing the burning particles in air, steam or SF_6, film with film speed of ASA 200 was used. The column labeled "Time Particle Radiates" provides the average values obtained from many tracks observed in many experiments. Fig. 5b discussed earlier

gives a histogram of burning time. Burning time in these experiments equals the time that particle was observed by the film.

Using the chopper, the particle velocity can be measured. The initial velocity at which the particles are ejected from the wire are given in Table 4. Particles ejected from wire rupture in vacuum tend to be longer (fewer particles) moving at a smaller velocity. Particles formed in steam have the highest velocity.

A description of the plasma is given in Table 4 as well as notes concerning particle behavior.

Finally, the average value for initial track width is given for cases of particles formed in steam and SF_6. The track width differs from the particle diameter by the size of the flame. Fig. 5a provides a histogram of initial track width; these data are for many tracks from a few experiments.

B. Model for Combustion Rate and Particle Temperature

Using the simpified model for the burning of a single droplet of fuel that was made by Goldsmith and Penner [9] and using equation (24) from page 282 of Goldsmith and Penner:

$$\dot{m} = \frac{4\pi\lambda}{C_p} \frac{\ell n[1 + \frac{C_p}{L}(T_c - T_p)]}{\frac{1}{r_p} - \frac{1}{r_c}} \tag{4}$$

where $\dot{m}$ - steady-state mass rate of fuel consumption

λ - thermal conductivity of aluminum =237 @ $\frac{\text{watt}}{\text{cm}^\circ\text{C}}$ 300 K

C_p - specific heat of aluminum = 0.26 $\frac{\text{cal}}{\text{gm}^\circ\text{C}}$ @ 2000 K

L - specific latent heat and aluminum = 95 $\frac{\text{cal}}{\text{gm}}$

T_c - combustion temperature = 3000 K

T_p - temperature on the particle surface

r_p - radius of the particle

r_c - radius of combustion zone

ρ - aluminum density = 2.7 gm/cm^3

Equation (4) can be rewritten in different way by using the measured terms of r_c, $\dot{r}_c$, T_c and by assuming that $m = 4\pi\rho r_p{}^2 . \dot{r}_p$ as follows:

$$T_p = T_c - \frac{L}{c_p} [\exp (\frac{\alpha-1}{\alpha^3} \frac{C_p}{\lambda} \rho . r_c \dot{r}_c) - 1] \tag{5}$$

where

$$\alpha = \frac{r_c}{r_p} > 1.$$

Define a parameter $$\chi = \frac{\alpha-1}{\alpha^3} \frac{C_p \rho r_c \dot{r}_c}{\lambda} \tag{6}$$

By using the variation of α from 1 to 2, the following results for χ could be obtained:

$$0 < \chi < 0.00124$$

where
$$\dot{r} = 0.6 \text{ cm/s},$$
$$r_c = 0.0142 \text{ cm}$$
$$T_c = 2800°\text{C}$$
$$1 < \alpha < 2$$

Using the above result for χ in equation (5) leads to the result that the particle temperature (T_p) is almost equal to combustion temperature (T_c) or $T_c > T_p$. Further, using this result in equation (4) shows that $r_c > r_p$.

By applying the same model for a conventional fuel as benzene, using the known following characteristics:

$$C_p(\ell) = 32.4 \text{ cal/gK } [5]$$

$$\lambda = 2.87 \times 10^{-4} \text{ cal/scmK } [5]$$

$$L = 131.5 \text{ cal/g } [5]$$

$$\rho = 0.88 \text{ g/cm}^3 \ [5]$$

$$\alpha \approx 9 \ [9]$$

$$T_c = 3200 \text{ K } [9]$$

Assuming that $\dot{r}_c$ for the benzene will be the same as measured for aluminum combustion in SF_6 atmosphere (0.6 cm/s), the factor X equals 6.5 and T_p equals to 510 K. This result is comparable to the results in Goldsmith and Penner [9]. Therefore, according to this model, one can conclude that the combustion of aluminum particles in SF_6 atmosphere takes place on the surface or close to the surface of the particle.

C. Conclusions

Listed below is the summary of experimental observations and a fact concerning the energy release due to aluminum combustion in SF_6 compared to combustion in air or steam.

a) According to stoichometric equation, the reaction in SF_6 is more exothermic than in steam.

b) No oxide coating on aluminum particles (pure aluminum) burning in SF_6.

c) Decrease in track size along all the tracks in SF_6.

d) Long burning time in SF_6 compared to combustion in steam and in air.

e) Smaller size of the track width in SF_6 compared to steam.

f) Lower combustion temperature in SF_6 than in air and steam.

According to (a) one might expect a faster reaction rate in SF_6 than in steam, but the observations in (d) and (e) indicate lower rate of burning than in steam. Hence, one can anticipate that different mechanism of burning occurs

in SF_6 than in steam. The measured temperature in SF_6 (T_m) that is higher than T_{bo} (vapor temperature of $A\ell F_3$) indicates that sublimation of $A\ell F_3$ occurs in the reaction zone.

The decrease in particle size along the track (c) and the absence of oxide coating on the particle surface (b) is evidence for the sublimation. There was found by Brzustowski and Glassman [8] and by many other investigators that aluminum combustion in air and in steam is a vapor phase combustion which is characterized by $T_{bm} < T_c < T_{bo}$, where T_{bm} is vapor temperature of the metal, T_c is the temperature of combustion, T_{bo} is the boiling temperature of the oxide. (For burning in SF_6, the oxide is $A\ell F_3$). Markstein [10] defined the surface burning by $T_c \approx T_{bo} < T_{bm}$.

According the measured temperatures for aluminum combustion in SF_6 and the model of combustion in Section B, the conditions are comparable except the result of $T_c \approx T_{bm}$.

Table 5. Summary of Relevant Data

		Temperature K
Melting Temperature of Aluminum	T_{mm}	923
Boiling Temperature of Aluminum	T_{bm}	2740
Boiling Temperature $A\ell F_3$	T_{bo}	1564
Measured Temperature	T_m	2750 ± 150

Assume the measured temperature, T_m , equals the flame temperature, T_c: this is not a critical assumption and is stated for purposes of discussion. The measured temperature range is from 2600 K to 2900 K. If the actual T_c is 2600 K, then surface burning occurs. If the actual T_c is 2900 K then vapor phase burning is consistent with the observations.

Arguments can be given for surface burning. According to Table 4 the

rate of burning of aluminum in SF_6 is 0.4 times the rate of burning in steam. Particles formed in SF_6 tend to be smaller than those formed in steam; see Table 4. Adjusting burning rate for particle diameter, the value of 0.4 for the ratio of rates is even smaller. This fact is indicative of surface burning but is not conclusive.

According to Section B, the fact that $r_c \approx r_p$ is consistent with $T_c \approx T_p$ and with a vapor phase reaction. A controlling rate is heat transfer to the particle which is approximately

$$\dot{q} = \frac{\dot{m}L}{A} \approx \frac{\lambda}{A} \frac{T_c - T_p}{r_c - r_p} \tag{7}$$

where A is the surface area of an aluminum particle, and $\dot{q}$ is heat flux in J/s . Equation (7) indicates that when $T_c \approx T_p$, then $r_c \approx r_p$.

In Fig. 10 there is logical flow graph for determining the combustion process.

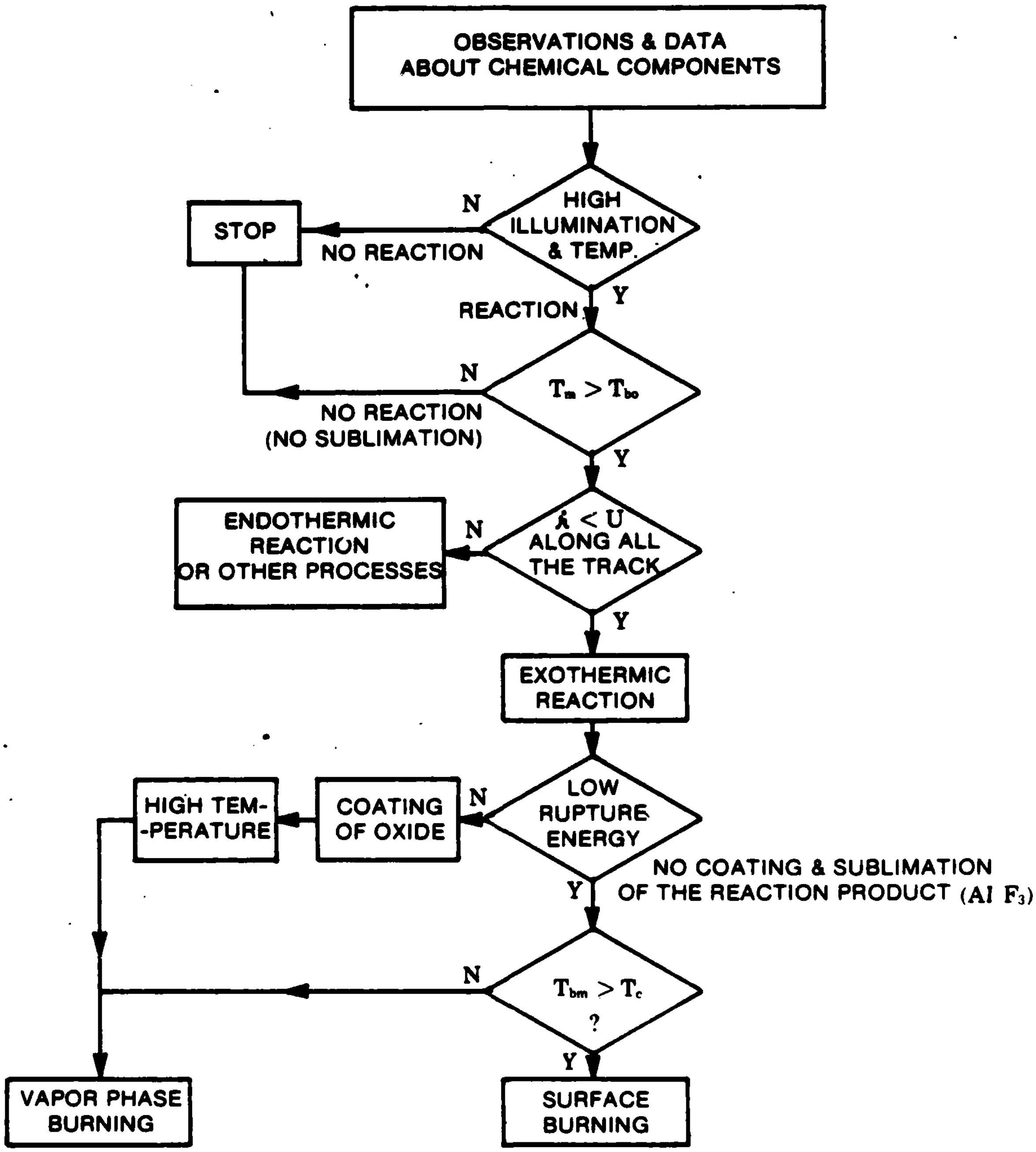

Figure 10. Logical Flow Graph Determining the Combustion Process

V. LIST OF REFERENCES

1. Cook, E. and Siegel, B., Reactions of Sulfur Hexafluoride with Exploding Metals, J. Inorg. Nucl. Chem., Volume 29/11, pp. 2739-2743, 1967.

2. Grigor'eva, A. A., Danilkin, V. A., and Bondarev, B. I., Onrabotka Alyuminievykh Rasplavov Gazoobraznymi Ftoristymi Soedineniyami s Tsel'yu Snizheniya Soderzhaniya Vodoroda. (Treatment of Aluminum Melts With Gaseous Flourine Compounds for the Purpose of Reducing the Hydrogen Content), Tsvet Met, pp. 77-79, 5 May 1981.

3. Berger, M., Fuhs, A. E. and Kol, J., Two-Color Photo-Pyrometry Method for Temperature Measurement of Moving Burning Particles, Twenty Third AIAA Aerospace Sciences Meeting, AIAA85-0157, January 1985.

4. Chozev, Y. and Kol J., Burning Time and Size of Aluminum, Magnesium, Zirconium, Tantalum and Pyrofuze Particles Burning in Steam, Naval Postgraduate School Contractor Report, to be published.

5. Weast, R. C., Editor-in-Chief, CRC Handbook of Chemistry and Physics, 64th Edition, pp. 83-84, CRC Press.

6. Hoerner, S. F., Fluid Dynamic Drag, Hoerner Fluid Dynamics, Brick Town, NJ pp. 3-8, 1965.

7. Kol, J., Fuhs, A. E. and Berger, M., Experimental Investigation of Aluminum Combustion in Steam, Twenty Third AIAA Aerospace Sciences Meeting, AIAA85-0323, January 1985.

8. Brzustowski, T. A. and Glassman, I., Vapor Phase Diffusion Flames in the Combusiton of Magnesium and Aluminum, Heterogeneous Combustion, Academic Press, New York, Volume 15, pp. 75-116.

9. Penner, S. S., Chemistry Problems in Jet Propulsion, Pergamon Press, New York, Volume 1, pp. 277-282, 1957.

10. Markstein, G. M., Heterogeneous Reaction Process in Metal Combustion, Eleventh (International) Symposium on Combustion, pp. 219-232, 1967, Combustion Institute, Pittsburgh, Pennsylvania.

DISTRIBUTION LIST

		No. Copies
1.	Defense Technical Information Center Cameron Station Alexandria, Virginia 22314	2
2.	Library, Code 0142 Naval Postgraduate School Monterey, California 93943	2
3.	Department Chairman, Code 67 Department of Aeronautics Naval Postgraduate School Monterey, California 93943	1
4.	Distinguished Professor Allen E. Fuhs Code 67Fu Naval Postgraduate School Monterey, California 93943	2
5.	Mr. Donald E. Phillips, Code R10A White Oak Laboratory Naval Surface Weapons Center Silver Springs, Maryland 20910	3
6.	Dr. Franklin D. Hains, Code R14 White Oak Laboratory Naval Surface Weapons Center Silver Springs, Maryland 20910	1
7.	Mr. Wayne K. Reed, Code R14 White Oak Laboratory Naval Surface Weapons Center Silver Springs, Maryland 20910	1
8.	Information Services Division, Code X20 White Oak Laboratory Naval Surface Weapons Center Dahlgren, Virginia 22448	1
9.	Mr. George Daniello White Oak Laboratory Naval Surface Weapons Center Silver Springs, Maryland 20910	1
10.	Captain Robert M. Wellborn, Jr., Director Mark 50 Torpedo Office Naval Sea Systems Command Washington, DC 20360	1

11. Mr. Francis J. Romano, SEA 63R3 1
Naval Sea Systems Command
Washington, DC 20360

12. Dr. William Sykes, Code 175 1
David W. Taylor Naval Ship Research
and Development Center
Bethesda, Maryland 20084

13. Mr. Raymond P. Gogolewski 1
Defense Advanced Research Project Agency
1400 Wilson Boulevard
Arlington, Virginia 22209

14. Mr. Charles Beatty 1
Naval Undersea Center
San Diego, California 92132

15. Professor Forman Williams 1
Princeton University
Princeton, New Jersey 08540

16. LCDR Amos E. Hallenbeck, Jr. 2
3293 Edinburgh Drive
Virginia Beach, Virginia 23452

17. Jonathan L. Minner 1
Naval Surface Weapons Center
Dahlgren, Virginia 22448

18. Zernow Technical Services 1
Attn: Louis Zernow
425 West Bonita
San Dimas, California 91773

19. Dr. Louis Baker, Jr. 1
Argonne National Laboratories
9700 South Cass Avenue
Building 207
Argonne, Illinois 60439

20. Professor Irvin Glassman 1
Department of Mechanical and
Aeronautical Engineering
Princeton University
Princeton, New Jersey 08540

21. R. G. S. Sewell 1
Code 3835
Naval Weapons Center
China Lake, California 93555

22. R. R. Durrell 1
Code R12
Naval Surface Weapons Center
Silver Springs, Maryland 20910

23. LT Jerome Buck 1
USS Goldsborough (DDG-20)
FPO, San Francisco 96666

24. LT John Strott 1
USS Radford (DD-968)
FPO, New York 09586

25. D. R. Kennedy Associates, Inc. 1
4940 El Camino Real, Suite 209
Post Office Box 4003
Mountain View, California 94040

26. Mr. J. M. McNerney 1
Battelle
Columbus Laboratories
505 King Avenue
Columbus, Ohio 43201

27. Dr. G. E. Jensen 1
Chemical Systems Division
United Technology Corporation
Post Office Box 358
Sunnyvale, California 94086

28. Dr. Edward G. Liszka 1
Mark 50 Torpedo Office
Naval Sea Systems Command
Washington, DC 20360

29. Mr. Mati Berger 1
Ministry of Defense
P.O. Box 2250
Haifa, Israel

30. Mr. Jacob Kol (88) 1
Ministry of Defense
P.O. Box 2250
Haifa, Israel

31. Professor C. K. Law 1
Department of Mechanical Engineering
University of California at Davis
Davis, CA 95616

32. Mr. Yair Chozev 1
Ministry of Defense
P.O. Box 2250
Haifa, Israel

33. Professor A. Gany 1
Department of Aeronautical Engineering
Technion - Israel Institute of Technology
Haifa, Israel

34. Dr. Norman Hubele 1
Mail Stop 1301-R
GPSD
2801 E. Washington
Phoenix, AZ 85034

35. Professor Paul Dimotakis 1
California Institute of Technology
301-46
Pasadena, CA 91125

36. Research Administration Office 1
Code 012A
Naval Postgraduate School
Monterey, CA 93943

END

FILMED

10-85

DTIC